Cell Reports

Article

The balance between conventional and unconventional T follicular helper cells influences autoreactive B cell responses

Graphical abstract

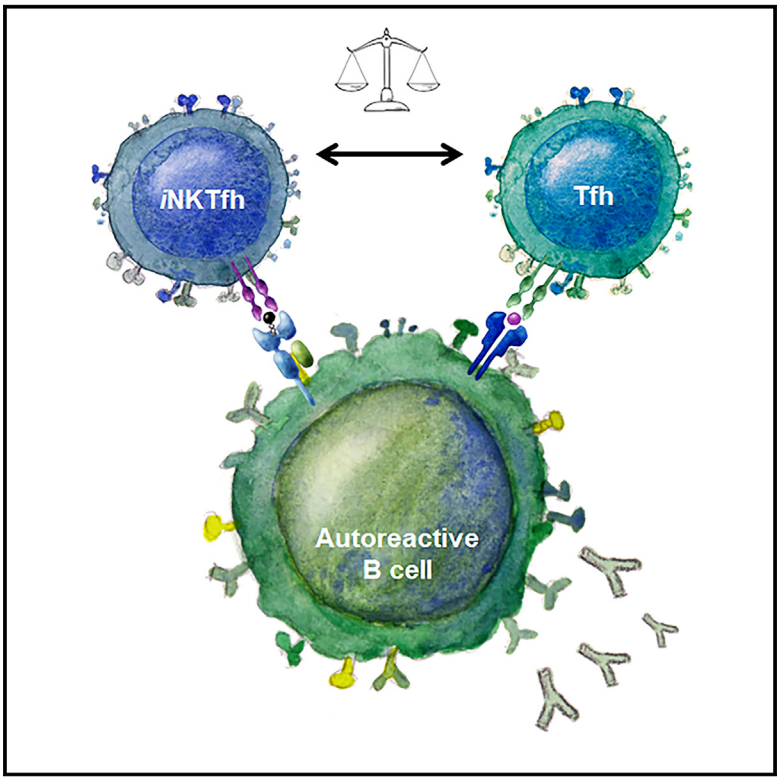

Authors

Chenfei He, Shan Wang, Marion Moreews, ..., Marcus Buggert, Facundo D. Batista, Mikael C.I. Karlsson

Correspondence

mikael.karlsson@ki.se

In brief

In this study, He et al. find that there is a balance between conventional and unconventional T helper cells and that this influences autoreactive B cell responses. They find that when iNKTfh cells are activated, they limit the expansion of Tfh cells, but the resulting autoreactive B cell response is increased.

Highlights

- Conventional and unconventional T follicular helper cells influence each other
- Autoreactive B cell responses are enhanced by the activation of *i*NKTfh cells
- Activation of *i*NKTfh cells is connected to interaction with CD1d expressed by B cells

He et al., 2025, Cell Reports *44*, 115602
May 27, 2025
https://doi.org/10.1016/j.celrep.2025.115602

CellPress

Cell Reports

CellPress
OPEN ACCESS

Article

The balance between conventional and unconventional T follicular helper cells influences autoreactive B cell responses

Chenfei He,[1,9] Shan Wang,[1,9] Marion Moreews,[1] Shengduo Pei,[1] Guangchun Chen,[2] Quan-Zhen Li,[2] Alberto Del Monte Monge,[3] Almudena R. Ramiro,[3] Curtis Cai,[4] Mauro Gaya,[5] Patricia Barral,[6,7] Marcus Buggert,[4] Facundo D. Batista,[8] and Mikael C.I. Karlsson[1,10,*]

[1]Department of Microbiology, Tumor and Cell Biology, Karolinska Institutet, Tomtebodavägen 16, Solna Campus, 171 65 Stockholm, Sweden
[2]Microarray Core, Department of Immunology, University of Texas Southwestern Medical Center, Dallas, TX 75390, USA
[3]Spanish Center for Cardiovascular Research, Melchor Fernandez Almagro 3, Madrid, Spain
[4]Center for Infections Medicine, Department of Medicine Karolinska Institutet, Huddinge, Sweden
[5]Centre d'Immunologie de Marseille-Luminy (CIML), Aix Marseille Université, INSERM, CNRS, Marseille, France
[6]The Francis Crick Institute, London, UK
[7]Center for Inflammation Biology and Cancer Immunology, The Peter Gorer Department of Immunobiology, King's College London, London, UK
[8]Ragon Institute of MGH, MIT, and Harvard, 400 Technology Square, Cambridge, MA 02139, USA
[9]These authors contributed equally
[10]Lead contact
*Correspondence: mikael.karlsson@ki.se
https://doi.org/10.1016/j.celrep.2025.115602

SUMMARY

Invariant natural killer T (*i*NKT) cells are activated by glycolipids presented on CD1d. When *i*NKT cells interact with and activate B cells, they can differentiate into *i*NKT follicular helper (*i*NKTfh) cells, and here, we investigate how this, in turn, regulates conventional T follicular helper (Tfh) cells. This is done in an autoimmune model where antibodies are produced against self-antigens relevant to the autoimmune disease systemic lupus erythematosus (SLE). We find a balance between *i*NKTfh and Tfh cells that directs the B cell response and influences Tfh cell generation. This altered balance also affects the specificities and increases the autoantibody response. We also show that CD1d expression by B cells is essential for *i*NKTfh cell generation. In conclusion, our data shed light on how T cell help for B cells is divided between conventional and unconventional helper cell populations and how this has an impact on autoreactive B cell responses.

INTRODUCTION

Antibodies against self-antigens are the drivers of autoimmune disease and disrupt normal immune function, form immune complexes, and cause inflammation and tissue destruction. In a healthy immune system, B cell tolerance is maintained through two checkpoints. The first is during development in the bone marrow, where autoreactive clones are deleted, while the second is in the periphery, regulated by interactions with T cells.[1,2] During the adaptive immune response, B cells differentiate into plasma cells directly through an extrafollicular response or by being selected in the germinal centers (GCs) after somatic hypermutation, giving them a higher affinity for their antigen. Although class switching and some somatic hypermutation have been shown, the extrafollicular response primarily triggers the production of immunoglobulin (Ig)M or IgG3 subclasses with low affinity. In contrast, the GC response mainly generates IgG-producing B cells with high affinity.[3–5] The activation of B cells to enter these two pathways is regulated by T follicular helper (Tfh) cells that provide help for B cells and are also the limiting factor for selecting B cells and the magnitude of the GC response.[6] Interaction with B cells and upregulation of the transcription factor Bcl-6 and follicle-homing induced by the chemokine CXCR5 are essential for forming Tfh cells. Mature Tfh cells further upregulate molecules needed to interact with B cells or support their growth, including PD-1, CD40L, ICOS, SAP, and interleukin (IL)-21.[7,8]

In addition to conventional T cells, it has also been shown that unconventional T cells, including invariant natural killer T (*i*NKT) cells, can provide help to B cells and differentiate into *i*NKT follicular helper (*i*NKTfh) cells.[9,10] Unlike conventional Tfh cells, *i*NKT cells recognize glycolipid antigens presented on the major histocompatibility complex (MHC) class 1-like molecule CD1d. They are also characterized by a limited T cell receptor (TCR) repertoire using the α chain Vα14-Jα18 and the β chain Vβ2,7 or -8 in mice. The glycolipid antigens that activate *i*NKT cells can be either foreign or self. As a source for self-glycolipids, it has been shown that cellular stress responses in dendritic cells (DCs) induce modification of intracellular glycolipids that can be presented on CD1d to *i*NKT cells.[11] *i*NKTfh cells can also become memory cells and activate B cells during recall

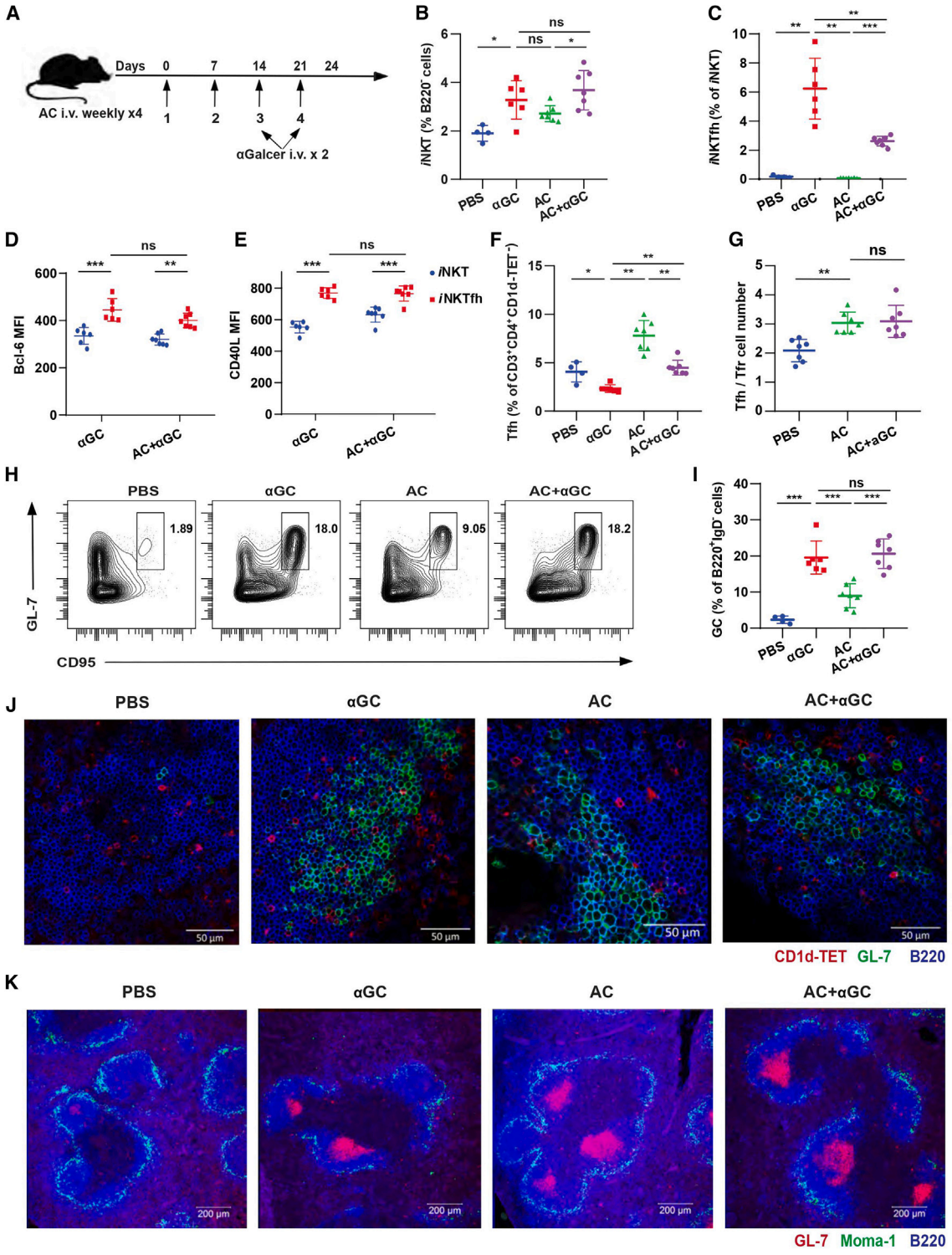

Figure 1. Glycolipid-activated *i*NKTfh cells negatively impact the formation of AC-induced Tfh cells

(A) A graphical scheme with a timeline of the mice experiments. Age- and sex-matched C57BL/6 wild-type mice were administered intravenously (i.v.) with AC weekly for 4 weeks, and 2 μg αGalCer (αGC) was added at the 3rd and 4th injections. Control groups include ACs alone, αGC alone, and PBS. Spleens were collected 3 days after the last administration.

(B) The frequency of splenic *i*NKT cells ($CD3^+CD1d\text{-}TET^+$) (TET, tetramer) of $B220^-$ cells.

(C) Frequency of splenic *i*NKTfh ($CXCR5^+PD\text{-}1^+$) in *i*NKT cells.

(legend continued on next page)

responses.[12] The most used foreign glycolipid to study *i*NKT cells is α-galactosylceramide (αGalCer), and it induces both cognate and non-cognate *i*NKT cell help to B cells. On the one hand, cognate *i*NKT cell help is given by direct interaction with CD1d-expressing B cells and can generate both GC B cells and plasma cells but with limited affinity maturation and no memory.[13,14] On the other hand, the non-cognate *i*NKT cells support B cells by interacting with antigen-presenting cells (APCs) that prime Tfh cells.[15] In contrast to this, *i*NKT cells can also negatively regulate B cell activation through a mechanism where they get licensed by neutrophils.[16] In addition, direct interaction between *i*NKT cells and B cells can lead to the activation of B cells to secrete IL-10, and these cells have been shown to regulate autoimmunity negatively. Thus, whether *i*NKT cells support B cell activation or mediate suppression is context dependent, and in general, glycolipids inducing strong interactions will enhance the response.[17] In connection to human autoimmune disease, patients with systemic lupus erythematosus (SLE) have lower numbers of *i*NKT cells in circulation and decreased CD1d expression in B cells, which has been linked to increased internalization of CD1d by B cells.[18] This phenotype is disease driven, as treatment with rituximab that depletes B cells restores both *i*NKT cell numbers and CD1d levels on B cells upon their return after treatment. Also, in experimental systems, *i*NKT cells inhibit autoreactive B cells using a mouse model where autoantibodies are induced by injecting apoptotic cells (ACs).[19] Thus, even though the activation of both Tfh and *i*NKTfh cells is present during autoreactive B cell activation, it is unclear how the two populations influence each other.

It is known that conventional Tfh cells are clonally selected during the GC reaction and are the limiting factor for B cell selection,[20] but how *i*NKTfh cells control and if they influence this process have not been explored. Thus, we sought to examine how the balance between Tfh and *i*NKTfh cells regulates autoreactive B cell responses. To do this, we applied a mouse model where repeated injection of syngeneic ACs breaks the self-tolerance and triggers the production of autoantibodies with reactivities relevant to SLE.[21] To activate and differentiate *i*NKT cells to an *i*NKTfh phenotype, we co-administered ACs with the glycolipid αGalCer or an analog (OCH) that stimulates a more Th2-biased cytokine production when activating *i*NKT cells.[22] The response was compared to either ACs alone or glycolipid alone. We found that activation of *i*NKTfh cells when injecting ACs and glycolipids triggered a response that promoted GC B cell development and autoreactive IgG production to a higher degree than AC alone. Also, the co-injection reduced the number of conventional Tfh cells while maintaining the GC response and plasma cell output. Using a model antigen to measure affinity maturation of the antibody response, we found evidence of increased affinity when glycolipids were co-administered during immunization. Conditional targeting of CD1d in B cells showed that direct cognate interaction is involved in the generation of *i*NKTfh cells, GC B cells, plasma cells, and autoantibody production. Thus, we here describe a balance between Tfh and *i*NKTfh cells in regulating autoreactive B cell responses. This balance has an impact on which B cells are activated and the magnitude of the GC response, as well as on which antibody subclasses are produced. These findings are significant for both B cell tolerance-connected SLE and infections, which trigger *i*NKT cell activation and could directly impact Tfh cell generation.

RESULTS

*i*NKTfh cells modify the T cell response to ACs

Injection of syngeneic ACs weekly for 4 weeks without an adjuvant breaks B cell tolerance to self-antigens in mice and causes an autoimmune response, including autoantibody production.[21] The response includes autoantibody specificities that are found in patients with SLE and used as part of their diagnosis.[23] The response is negatively regulated by *i*NKT cells, but whether and how the activation of *i*NKTfh cells modulates the response have not been investigated. To address this, we injected ACs weekly for 4 weeks and combined them with αGalCer at the 3rd and 4th injections (combo) (Figure 1A). The response was then compared with either vehicle control, AC, or αGalCer alone. We found that combo and αGalCer alone induced an influx of *i*NKT cells in the spleen, both as a percentage of lymphocytes and as absolute numbers (Figures 1B and S1A). To investigate the generation of *i*NKTfh cells, we determined the expression of CXCR5 and PD-1 by *i*NKT cells.[24] Mice that received αGalCer or combo showed increased splenic *i*NKTfh cell numbers, while we did not find these in the AC-alone or vehicle groups. Mice administered αGalCer alone also had more *i*NKTfh cells than the combination, showing that ACs decreased their formation (Figures 1C and S1B). Activation of *i*NKTfh cells like conventional Tfh cells includes the upregulation of Bcl-6 and co-receptors, including CD40L, ICOS, PD-1, IL-21, and SAP.[25] Since we previously found that *i*NKT cells can negatively regulate the response to ACs, we next investigated the activation status of *i*NKTfh cells in the response where αGalCer was injected together with ACs. We found that both the expressions of Bcl-6 and CD40L were upregulated in *i*NKT and *i*NKTfh cells and that there was no difference between the αGalCer and combo groups (Figures 1D and 1E).

(D and E) The mean fluorescence intensity (MFI) of Bcl-6 and CD40L in *i*NKTfh and *i*NKT cells.
(F) The percentage of splenic Tfh cells (CXCR5$^+$PD-1$^+$) of CD3$^+$CD4$^+$CD1d-TET$^-$ cells.
(G) Frequency of splenic Tfh cells vs. Tfhr cells (CXCR5$^+$PD-1$^+$Foxp3$^+$).
(H and I) Representative fluorescence-activated cell sorting (FACS) contour plots and frequency of splenic GC B cells (CD95$^+$GL-7$^+$) of B220$^+$IgD$^-$ cells from mice 3 days after the 4th AC injection.
(J) Visualization of *i*NKT cells in the spleen section. CD1d-TET$^+$ *i*NKT cells (red), GL-7$^+$ GC B cells (green), and B220$^+$ B cells (blue) were detected by fluorescence microscope.
(K) Visualization of GC in the spleen section. GL-7$^+$ GC B cells (red), Moma-1$^+$ marginal metallophilic macrophages (green), and B220$^+$ B cells (blue) were detected by fluorescence microscope.
Data are representative of three independent experiments. *$p < 0.05$, **$p < 0.01$, ***$p < 0.001$, and ns: not significant (Mann-Whitney test).

It is known that the injection of αGalCer alone induces a GC response but that it is not mature, with limited class switching, and that it fades quickly.[17] In line with this, we found that there were no Tfh cells found in the αGalCer group. However, mice receiving the combination of αGalCer+ACs formed fewer Tfh cells compared with treatment with ACs alone, which suggested that the addition of αGalCer inhibited the formation of Tfh cells (Figures 1F and S1C). Thus, both Tfh cells and *i*NKTfh cells were recruited by co-administration, but both populations were reduced. The reduced number of Tfh cells made us investigate if there might be a difference in balance between Tfh and T follicular helper regulatory (Tfr) cells.[26] We found that both ACs and combo induced Tfr populations but that the relative numbers were not different (Figures 1G and S1G). The reduction of Tfh cells would suggest that the GC reaction would be reduced, as these have been shown to be a limiting factor. However, we found that the GL7- and CD95-positive GC cells were increased in the group receiving the combo as compared to ACs alone (Figures 1H and 1I). Thus, this showed that the activation of *i*NKTfh cells can support an equal or stronger GC response, even though the number of Tfh cells is reduced. Next, when investigating the GC response using immunofluorescence, we found tetramer-positive *i*NKT cells in the vicinity of or inside the GL7-positive GCs. We also found a small but significant accumulation of *i*NKT cells in the GC of the combo group (Figures 1J and S1D). In addition, the GC formation was found to be normal and at the T/B cell border in the follicles, and we found no evidence of an increased extrafollicular foci response (Figures 1K and S1E). Also, the areas of the GC structures were similar between the AC and combo groups (Figure S1F). Finally, there was a significant reduction of the GL7-positive and CD95-negative population in the spleen (Figure S1G). This population is comprised of unswitched memory cells and B cells in a state of early activation, and the data suggest that these are also recruited to the GC reaction in the combo group. Thus, altogether, these data show that a combination of ACs and αGalCer drives a mature and stronger GC response than ACs alone.

*i*NKTfh activation influences the TCR repertoire of Tfh cells in the response to ACs

Since we found that there was a balance between conventional and unconventional Tfh cell numbers in the group receiving the combination of αGalCer and ACs, we next investigated if the combined activation of Tfh and *i*NKTfh cells would influence the TCR usage of these populations. To do this, we purified Tfh cells and *i*NKTfh cells from spleens and sequenced their TCR repertoires. As expected, using Shannon's entropy as a measurement of diversity, we found that *i*NKT cells had an invariant TCR (CDR3α) repertoire that was not changed under combo immunization (Figures 2A and 2B). This confirms that type I *i*NKT cells are being recruited to the *i*NKTfh pool during both conditions and also that the combinatory injections had little impact on the non-fixed TCRβ usage. Meanwhile, we found that the overall usage of TCRα and TCRβ chains of Tfh cells was equally diverse and did not change between the groups (Figure 2C). The overlap in diversity was mimicked to some degree by looking at individual TCR usage of Tfh cells, where we found that there was the greatest level of clonal sharing between the AC and combo groups (Figures 2D–2F). We next directly considered the TCRβ sequences ranked in order of their proportion of their respective populations to understand how different clones may be recruited following treatment conditions. Both AC- and αGalCer-alone injections recruited shared clones, although most comprised a relatively small proportion of the overall population. By contrast, we identified that the major clones following combo treatment were also present following single AC or αGalCer injections, and notably, highly ranked clones from ACs were also among the highest-ranked clones in the combo condition (Figures 2G–2I). Collectively, these findings suggest that combo injection provides synergistic recruitment of specific Tfh clonotypes, with the strongest contribution arising from the response to ACs. Thus, these data show that the concomitant activation of Tfh and *i*NKTfh cells induces differential expansion and recruitment of Tfh-TCR repertoires. Collectively, these findings suggest that combo injection results in the recruitment of Tfh populations that closely resemble AC infection alone and that αGalCer does not dramatically redirect the repertoire of recruited Tfh cells.

Co-administration of ACs with αGalCer changes class switching and influences plasma cell responses

It has been shown that *i*NKTfh cells can induce short-lived plasma cells, and early in the GC response, B cell interactions with Tfh cells promote class switching.[13] Thus, we investigated plasma cell formation in the spleen and found that in line with previous studies, αGalCer alone induced immature GCs with little output of total plasma cells as opposed to injections with ACs (Figure 3A). Also, the overall numbers of plasma cells were similar between AC alone and AC+αGalCer, mimicking the GC response in these two groups. Investigating subclasses of the plasma cell response, we found no difference in IgM-positive plasma cells, but there was a reduction of IgG1-positive plasma cells in the combo group compared to ACs alone (Figures 3B, 3C, and S2A). Further, we found that the number of IgG2-positive cells remained unchanged, and there was a tendency for higher numbers of IgG3-positive plasma cells in the group receiving αGalCer together with ACs (Figures 3D, 3E, and S2B). Using immunofluorescence, we found IgG1/CD138-positive plasma cells in the red pulp after AC injections but fewer in the group that received αGalCer alone (Figures 3F and S2C). Thus, *i*NKTfh cells, in combination with Tfh activation, alter the balance between antibody subclasses and reduce the number of IgG1-positive plasma cells compared to the Tfh cell-driven response when ACs are given alone. This will, in turn, alter the balance of engaging activating and inhibitory Fcγ receptors and could drive a more pro-inflammatory response.[27]

iNKTfh activation enhances antigen-specific and self-reactive immune responses to ACs

The finding that there was a balance between Tfh and *i*NKTfh numbers and a shift of antibody subclasses made us hypothesize that there could also be a shift in autoantibody specificity. To evaluate the antigen specificity of the response, we administered mice with ACs weekly for 5 weeks, and αGalCer was added for the 3rd and 4th injections. Only ACs were used for the final injection to boost the response to enhance the response that was

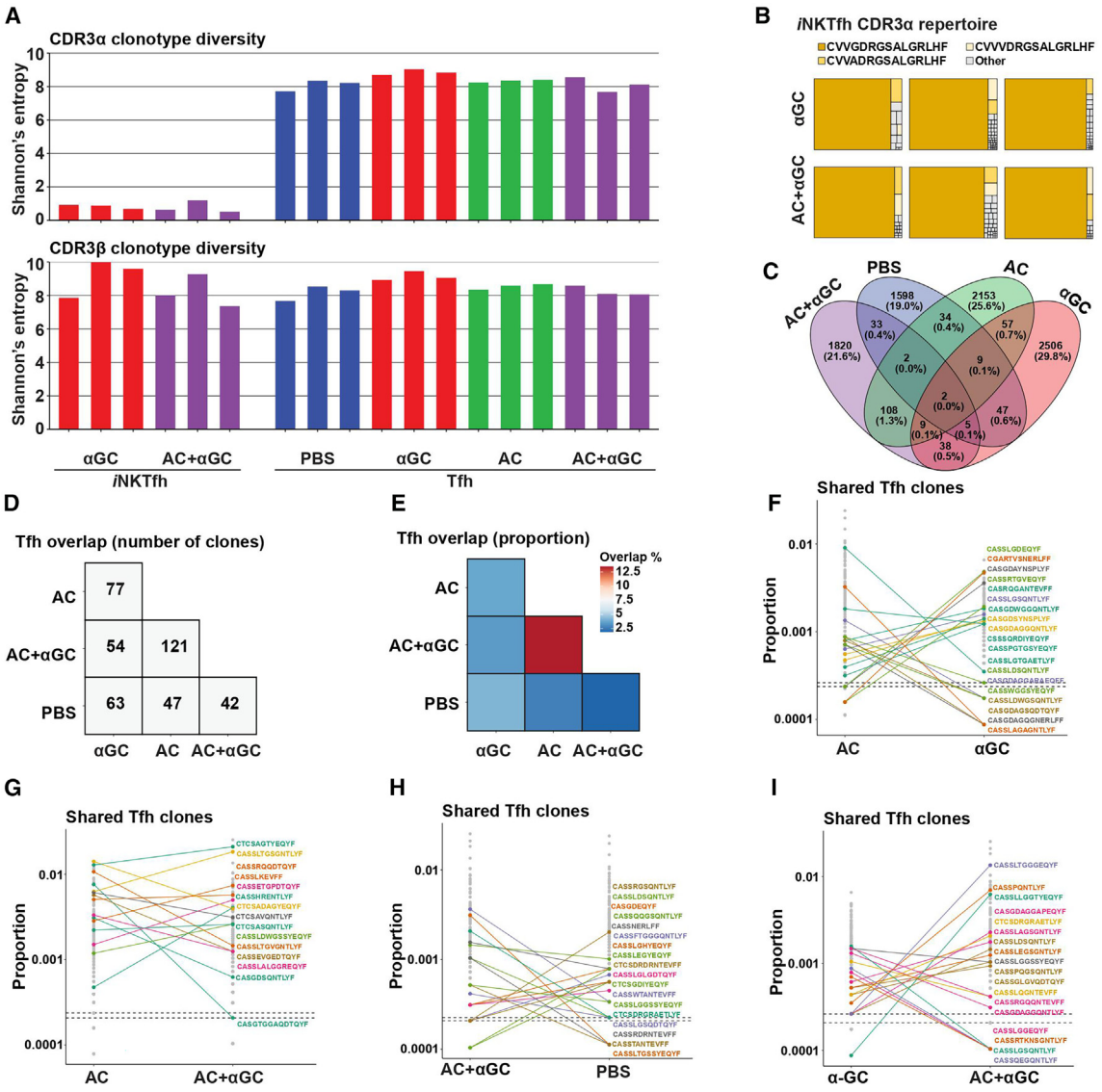

Figure 2. The repertoires of VDJ sequences from Tfh and *i*NKTfh cells

(A) Bar plot displaying CDR3α and CDR3β clonotype diversity measured by Shannon's entropy.

(B) TreeMap shows the composition of the CDR3α chain of *i*NKT cells.

(C) Venn diagram of overlapping TCR clones on Tfh cells between ACs and combo. Numbers represent the total number of shared clones and percentages.

(D and E) Heatmap showing the number and proportion of overlapping TCR clones on Tfh cells under treated conditions.

(F–I) Visualization of the frequency of overlapping TCR clones of Tfh cells among ACs and αGC, ACs and combo, combo and PBS, and αGC and combo. Gray dots are all TCR clones. The dotted lines are the median frequencies. Dots can be stacked so hundreds of TCR clones are sitting at the median. The proportion is out of 1 and plotted on a log scale. Only the top 10 clones from each population were selected, and some clones were in the top 10 in both populations.

modulated at the break of tolerance. Spleens and serum were collected 14 days after the last injection (Figure 4A). ACs induce an autoantibody response with many reactivities that are also found in patients with SLE.[28] One of these is antibodies against the phospholipid cardiolipin, which is a distinct class of autoreactive antibodies used for diagnosis.[29] Here, we used this antigen to investigate the kinetics of the response and found that after the first co-administration, there was a significant increase in serum IgG and IgG1 anti-cardiolipin, but this difference disappeared at later time points (Figures 4B and 4C). Next, serum collected from the last time point was used to investigate the autoantibody spectrum with autoantigen arrays containing 121 specificities. Both IgM and IgG1 autoantibodies were measured, and the autoantigens were divided into nuclear, cytoplasmic, and tissue-specific groups. We found that the addition of *i*NKTfh cell activation promoted higher levels of autoantibodies to most autoantigens, including protein and non-protein responses (Figures 4D–4F). We verified some of the specificities and found elevated IgG1 levels using ELISA against nucleolin, histone H3, histone H1, MPO, and complement C3a in the group receiving

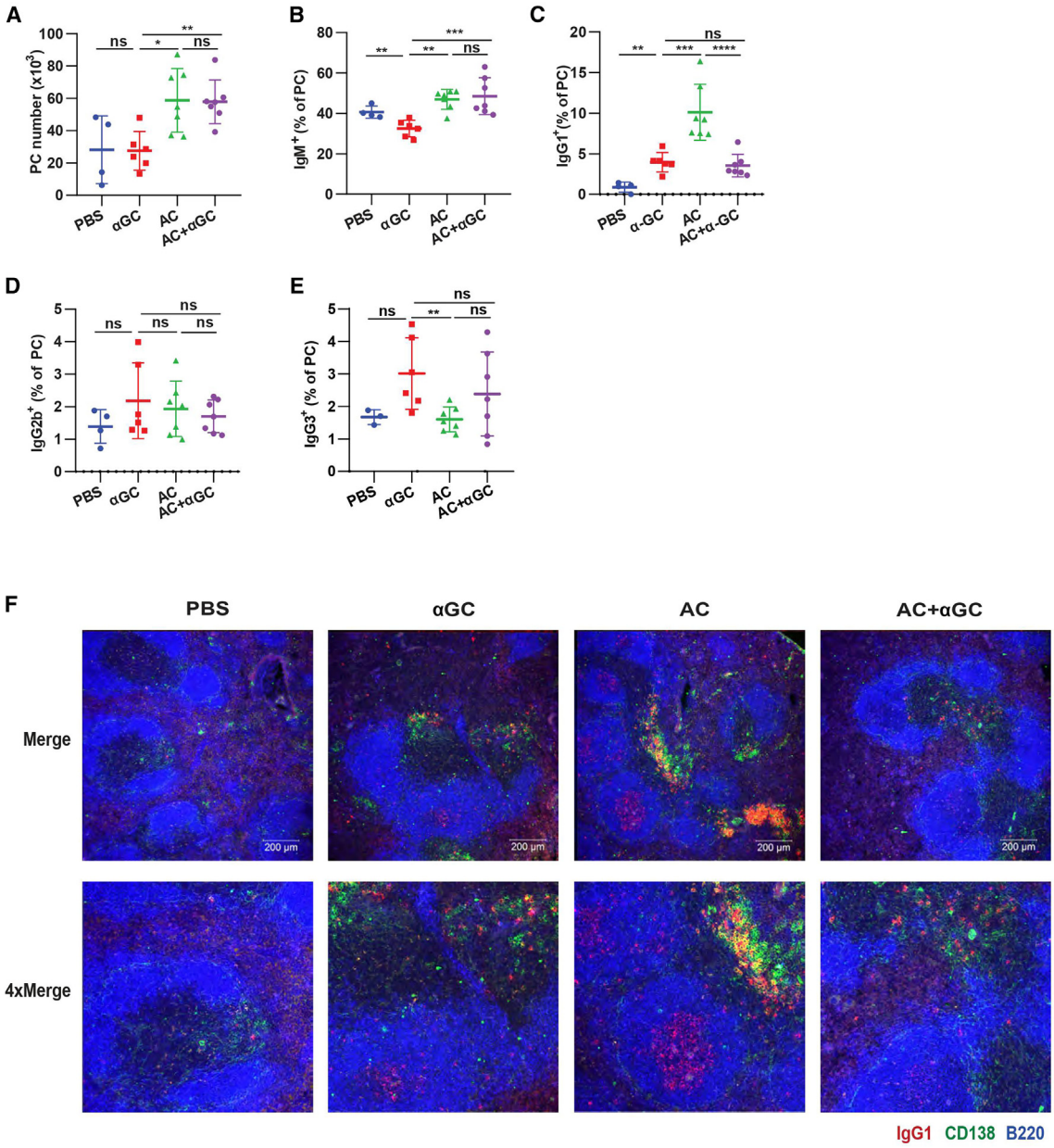

Figure 3. The competition of glycolipid-activated *i*NKTfh and conventional Tfh cells regulates the formation and class-switching of plasma cells

(A) The absolute number of splenic plasma cells (PCs) in live cells.
(B) Frequency of splenic IgM^+ PCs.
(C) The absolute number of splenic $IgG1^+$ PC.
(D and E) Frequency of $IgG2b^+$ and $IgG3^+$ PCs.
(F) Visualization of $CD138^+$ PCs and $IgG1^+$ PCs in the spleen section from the mice.
Data are representative of three independent experiments. $^*p < 0.05$, $^{**}p < 0.01$, and $^{***}p < 0.001$ (Mann-Whitney test).

the combination (Figures 4G–4K). We also found that αGalCer injection alone triggered autoreactive and polyreactive IgM antibodies (Figures S3A–S3C). However, these were not reactive with cardiolipin (Figure S3D). Although αGalCer induced a quick boost of autoreactive IgM, the response failed to switch into IgG1, most likely due to a lack of a mature GC reaction. Interestingly, though combinatory treatment with ACs and αGalCer showed little evidence for IgM autoreactivity. SLE disease is closely connected to and a co-morbidity of atherosclerosis, and recently, a novel target autoantigen, ALDH4, was found in this disease. ALDH4A1, as a mitochondrial dehydrogenase, is involved in proline metabolism.[30] Here, we found that the

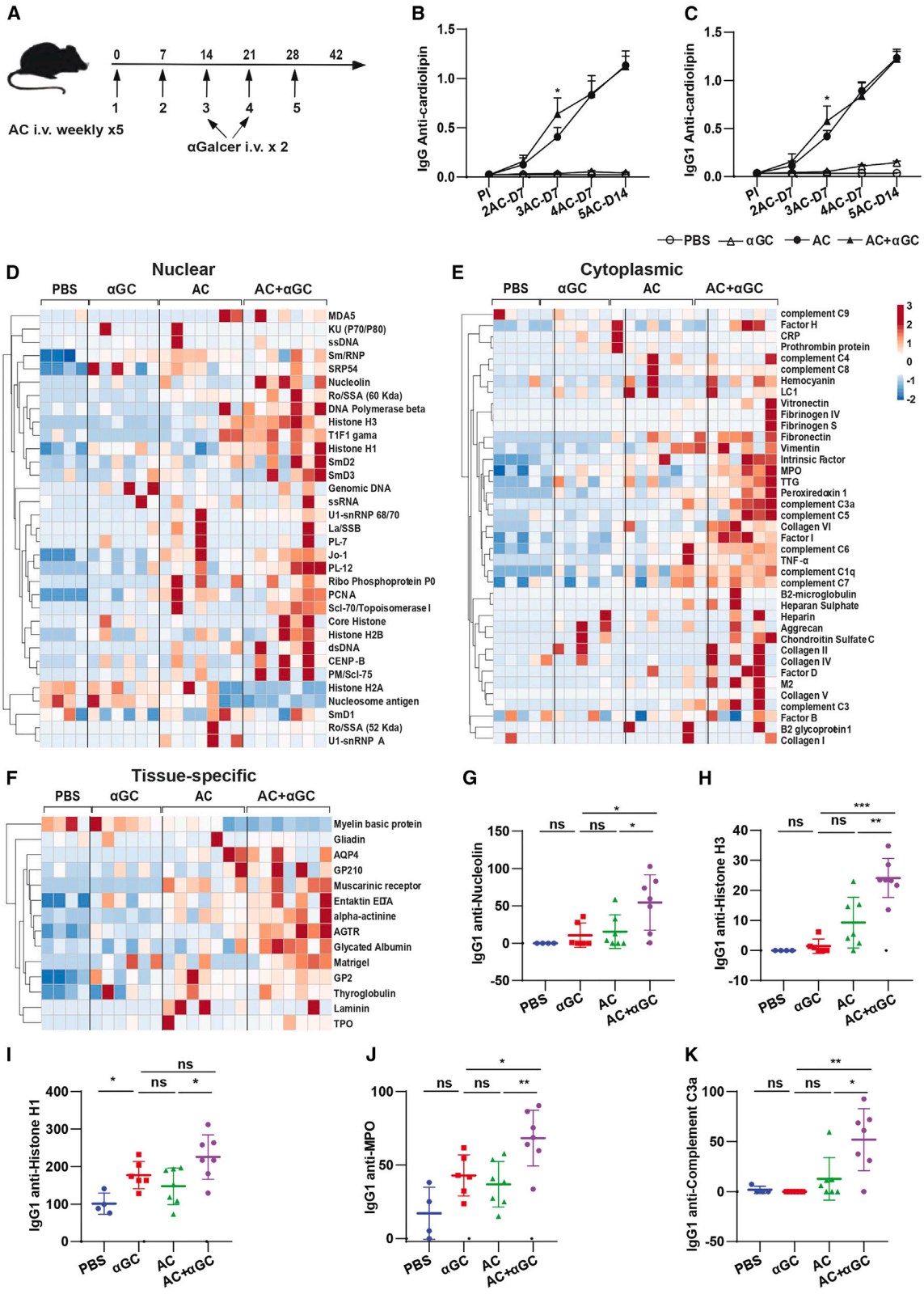

(legend on next page)

response to ALDH4 was induced by ACs and elevated with the addition of αGalCer. This was true for both IgM and IgG and implies an interesting connection to atherosclerosis, where modified glycolipids are an important part of driving the sterile inflammatory response (Figures S3E and S3F). When *i*NKT cells are activated by αGalCer displayed on CD1d, the cytokine response is known to include both interferon (IFN)-γ and IL-4. We hypothesized that this was, in part, the reason for the display of subclasses, and thus, we repeated the experiments using an αGalCer analog (OCH) that is known to give a more Th2-biased response. Using the same experimental setup, we found that OCH drove a similar phenotype in combination with ACs with the induction of *i*NKTfh cells and enhanced GC responses. Plasma cells were increased in numbers, and we found enhanced antibody responses to both cardiolipin and DNA. Unlike the experiments using αGalCer, however, we now find higher IgG2b and IgG2c responses with a shift in the balance toward more pathogenic antibody subclasses (Figures S4A–S4H). Thus, *i*NKTfh activation, in combination with a conventional Tfh cell activation, drives the generation of a broad spectrum of autoantibodies with reactivities that are also found in patients with SLE. Also, we find that the nature of the glycolipid influences the isotype switch of the autoantibody response. Next, we asked the question of whether *i*NKTfh activation in combination with Tfh activation could also drive affinity maturation. To test this, we used a model antigen (NP-CGG) where affinity can be measured as binding to the hapten NP. Mice were immunized with NP-CGG alone or in combination with αGalCer or OCH. When examining the resulting antibody response, we found that the addition of αGalCer or OCH increased the binding of the IgG2c response at days 7 and 14 (Figures S4I–S4K). Thus, the activation of *i*NKTfh cells increases the autoreactive antibody response and has the capacity to increase the affinity maturation of the GC.

Initial activation of *i*NKTfh cells and B cells requires CD1d expression and cognate interaction

Since *i*NKTfh cells activated by αGalCer alone did not drive a mature autoreactive GC response, but added to the AC-driven response, we hypothesized that the combination with AC would drive *i*NKT cells further into maturation and activation at an early stage of the response. In addition, we wondered if this was connected to cognate interactions with B cells. To investigate this, we injected wild-type (WT) mice with αGalCer, ACs, combo, or vehicle and investigated the activation of splenic B cells and *i*NKT cells after 24 h (Figure 5A). We found that both FOB and MZB downregulated their complement receptor CD21[31,32] and upregulated CD69[33,34] as a sign of activation (Figures 5B, 5C, and S5A–S5C). We also found the level of B cell activation to be comparable between αGalCer and combo groups, whereas the group receiving ACs alone did not show signs of activation. Next, to assess *i*NKT cell activation, we analyzed their expression of CD25 and PD-1. We found that the expression of both CD25 and PD-1 was upregulated after αGalCer or combo injection compared with ACs alone, and this was further enhanced when mice received the combo treatment (Figures 5D and 5E). It has been demonstrated that cellular stress can induce endogenous glycolipids to be presented on CD1d on DCs to activate *i*NKT cells.[11] Since the response to ACs and cell death in SLE is related to cellular stress and increased autophagy,[35] we next investigated whether stressed B cells would present endogenous ligands to *i*NKT cells. To test this, we used the innate B cell line CH12 that expresses CD1d and treated this with thapsigargin to induce a stress response *in vitro*. We found that when these cells were incubated together with the NKT cell hybridoma DN32.D3, we could detect IL-2 production as a measure of their activation (Figure 5F), and this was CD1d dependent (Figure 5G). In addition, naive B cells purified from the spleen could also activate the NKT cell hybridoma after induction of endoplasmic reticulum (ER) stress (Figure 5H). Thus, acute cellular stress can also make B cells activate *i*NKT cells. Just like for Tfh cells, the maturation of *i*NKTfh cells requires *i*NKT-B cell interactions. This was shown using transfers of $CD1d^{+/+}$ and $CD1d^{-/-}$ B cells when studying GC formation.[13] However, the early events of activation using mice with a specific deletion of CD1d in B cells have not been studied. To do this, we crossed mice carrying a floxed *Cd1d* allele ($Cd1d^{fl/fl}$) to mice expressing *Cre* recombinase under the control of *Mb1* promotor (*Mb1-Cre*), generating mice ($Cd1d^{fl/fl}$*Mb1Cre*) that delete *Cd1d* specifically in B cells.[10] In these experiments, $Cd1d^{fl/fl}$ mice were used as controls. At steady state, these mice had equal numbers of *i*NKT cells, showing that the deletion of CD1d in B cells did not alter *i*NKT cell development (Figure S5D). These mice were injected with αGalCer, and the response was investigated on day 10 (Figure 5I). We found that the specific knockout of CD1d in B cells greatly reduced early GC responses as compared to the control (Figures 5J and S5E). We also found that αGalCer injection increased *i*NKT cell numbers in the spleen and that this was reduced in the $Cd1d^{fl/fl}$*Mb1Cre* mice (Figure S5F). The formation of *i*NKTfh cells was also reduced, their expression of PD1 was lower, and we found no evidence of Tfh generation at this time point (Figures 5K, 5L, and S5G). This shows that the early recruitment of *i*NKTfh cells requires cognate interactions with B cells expressing CD1d. The injection of αGalCer alone induces little output of plasma cells (Figure S5H). However, we detected an accumulation of IgM- and IgG3-positive plasma cells, and these were significantly reduced in the conditionally targeted mice (Figures 5M and 5N). This also corresponded to reduced amounts of IgM and IgG3 levels in the serum (Figures 5O and 5P). Together, these results show that αGalCer initiates an early activation of both B cells and *i*NKT cells and that B cells can directly induce *i*NKT cell activation through cognate interactions, leading to an immature GC

Figure 4. αGalCer-activated *i*NKT cells modulate AC-induced autoimmunity

(A) Experimental scheme. C57BL/6 mice were injected i.v. with AC weekly for 5 weeks, and 2 μg αGalCer was added at the 3rd and 4th injections. Other immunogens and PBS were used as additional controls. Spleens and serum were collected 14 days after the last injection.

(B and C) ELISA was used to measure the OD_{450} of IgG and IgG1 anti-cardiolipin antibodies at various time points.

(D–F) Heatmaps present the serological spectrum of autoreactive IgG1 against nuclear antigens (D), cytoplasmic antigens (E), and tissue-specific antigens (F).

(G–K) The quantification of autoreactive IgG1 antibodies against nucleolin (G), histone H3 (H), histone H1 (I), MPO (J), and complement C3a (K).

Data are representative of three independent experiments. $^{*}p < 0.05$, $^{**}p < 0.01$, and $^{***}p < 0.001$ (Mann-Whitney test).

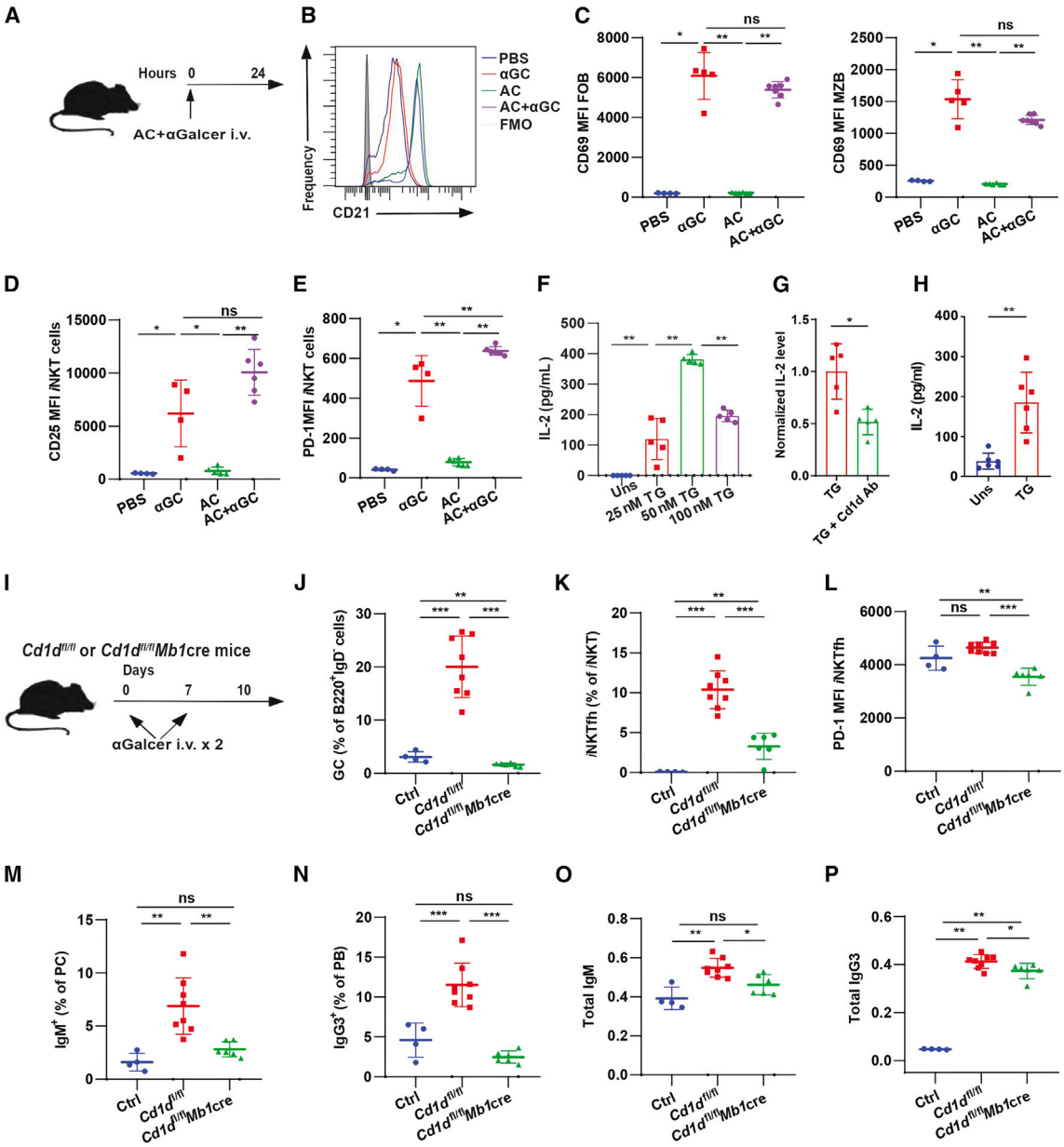

Figure 5. Administration of αGalCer initiates early activation of B and *i*NKT cells in a CD1d-dependent manner

(A) Experimental scheme. Mice were administered i.v. with 2 μg αGC alone, ACs alone, combo, or PBS, and spleens were collected 24 h after injection.

(B) Representative FACS histograms of CD21 staining in FOB and MZB.

(C) Quantification of CD69 staining in FOB and MZB.

(D and E) MFI of CD25 and PD-1 staining in *i*NKT cells.

(F) ELISA was performed to measure the IL-2 secreted by DN32.D3 under the interaction with CH12 cells (stimulated by 25, 50, and 100 nM thapsigargin).

(G) Normalization of IL-2 secreted by DN32.D3 under the interaction with CH12 cells stimulated by 25 nM thapsigargin with or without CD1d-blocking antibody.

(H) Measurement of IL-2 secreted by DN32.D3 under the interaction with primary B cells isolated from C57BL/6 mouse spleen.

(I) Age-matched *Cd1d*$^{fl/fl}$ and *Cd1d*$^{fl/fl}$*Mb1*cre mice were administered i.v. with 2 μg αGalCer weekly for 2 weeks, and spleens were analyzed 3 days after the last injection by FACS. *Cd1d*$^{fl/fl}$ mice did not receive any injection and serve as the littermate controls in experimental setups involving *Cd1d*$^{fl/fl}$*Mb1*cre mice.

(J) The frequency of splenic GC B cells (CD95^{+}GL-7^{+}) of B220^{+}IgD^{-} cells.

(K) The frequency *i*NKTfh cells (CXCR5^{hi}PD-1^{hi}) in *i*NKT cells (CD3^{int}CD1d-αGalCer tetramer^{+}).

(L) Quantification of PD-1 staining in *i*NKTfh cells.

(M and N) The frequency of IgM^{+} PC and IgG3^{+} PB.

(O and P) ELISA was used to measure the OD_{450} of IgM and IgG3 anti-IgG (H + L) antibodies.

Data are representative of three independent experiments. *$p < 0.05$, **$p < 0.01$, and ***$p < 0.001$ (Mann-Whitney test).

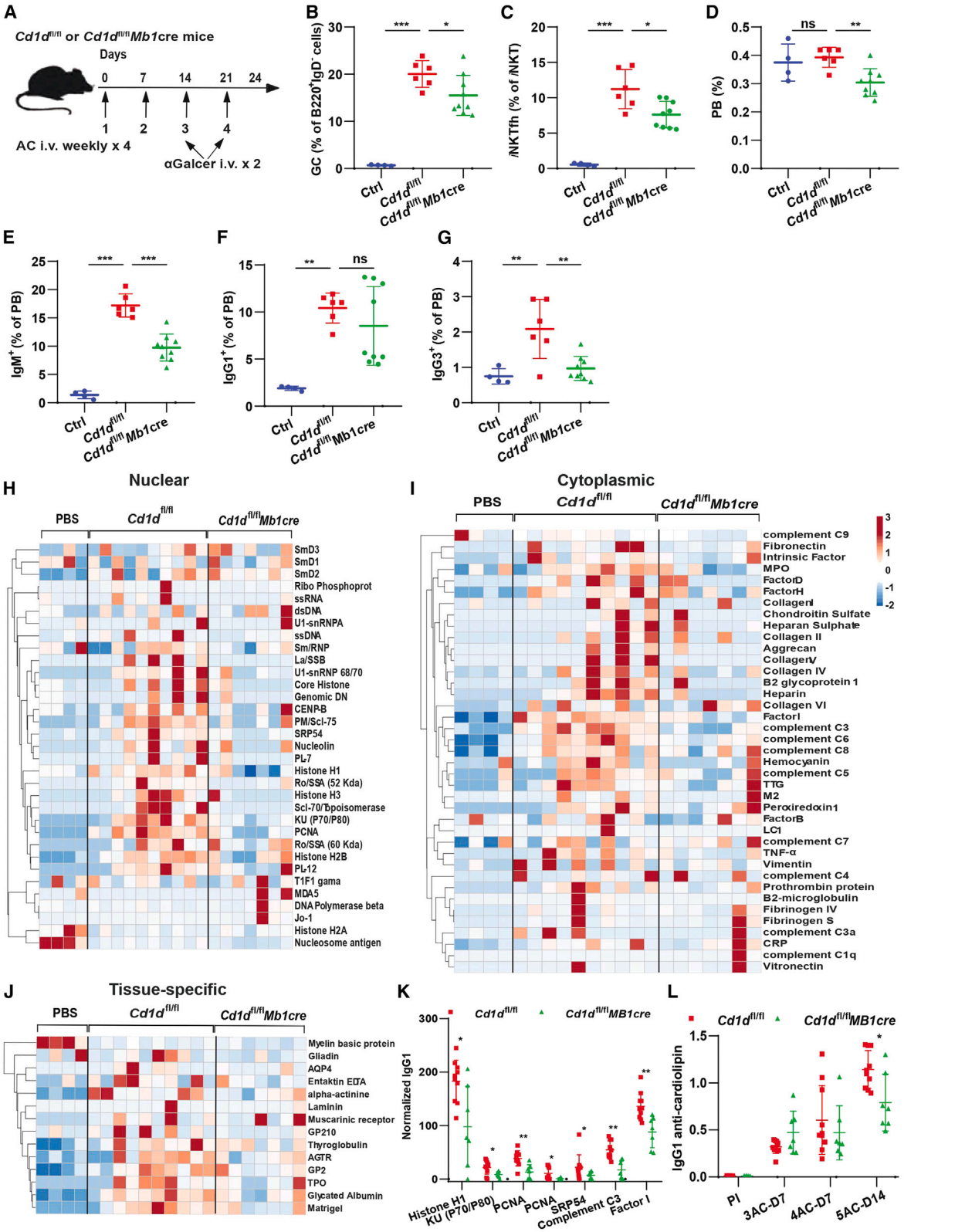

(legend on next page)

reaction. In addition, cellular stress can give rise to endogenous ligands on B cells that can activate NKT cells.

The absence of CD1d in B cells reduces the *i*NKTfh cell-regulated GC response to ACs

Having established the requirement for cognate interactions with B cells for the generation of *i*NKTfh cells, we next investigated the effect of specifically depleting CD1d in B cells for the generation of autoantibodies. Since we found that *i*NKTfh cells supported the generation of autoantibodies when ACs were used to break B cell tolerance, the question was if cognate interactions with B cells were needed for this. Thus, we injected *Cd1d*$^{fl/fl}$ and *Cd1d*$^{fl/fl}$*Mb1Cre* mice with ACs combined with αGalCer (Figure 6A). We found that in the absence of CD1d expression on B cells, there was significantly less GC formation compared with WT mice based on absolute numbers (Figures 6B and S6A). The generation of *i*NKTfh cells was also impaired in mice in the absence of CD1d in B cells (Figures 6C and S6B). Furthermore, there was a significant reduction in the formation of total plasma cells and also IgM, IgG1, and IgG3 positive both in frequency and absolute numbers (Figures 6D–6G and S6C–S6F). We next performed an autoantigen array to investigate whether these differences were true for the autoantibody response across all types of autoantigens. We found that the IgG1 response to most autoantigens was lower in mice lacking CD1d in B cells, suggesting that the decrease was general (Figures 6H–6J). It was also true for specific responses against histone H1, KU(P70/80), PCNA, SRP54, complement C3, and factor I (Figure 6K). The response was also lower against cardiolipin, as determined using ELISA (Figure 6L). The decrease in autoreactivity was also seen for auto-IgM, where we found that mice lacking CD1d in B cells had overall lower responses (Figures S6G–S6I). However, no significant difference in IgM autoantibodies against cardiolipin was observed between WT and *Cd1d*$^{fl/fl}$*Mb1Cre* (Figure S6J). Together, these data suggest that CD1d in B cells and cognate interactions are involved in the *i*NKTfh cell-driven autoimmune response.

Signaling through endosomal TLRs promotes the development of *i*NKTfh cells in response to ACs

Endosomal pattern recognition receptors Toll-like receptor (TLR) 3, TLR7, and TLR9 are essential sensors of cell death and signal through regulation by Unc93b1, which traffics these nucleotide-sensing TLRs to endosomes from the ER.[36] We have previously reported that mice lacking Unc93b1 have a lower response to ACs alone.[28] Here, we now investigated if endosomal TLRs also affected the regulation and generation of *i*NKTfh cells in the context of ACs together with αGalCer, thus investigating if endosomal pattern recognition was also essential under these conditions. First, WT and Unc93b1$^{3d/3d}$ mice were injected with αGalCer alone, and we investigated the *i*NKTfh-mediated immature GC response (Figure S7A). We found no difference in the numbers of GC B cells, *i*NKTfh cells, or plasma cells (Figures S7B–S7G). Next, we investigated the effect of knocking out endosomal pattern recognition on the response when injecting ACs alone or together with αGalCer (Figures 7A and S7H). As was previously shown, knocking out Unc93b1 led to less formation of GC B cells (Figures 7B and S7I), and the percentage of the Tfh population was lower (Figures 7C and S7J). We also found fewer *i*NKTfh cells and switched and unswitched plasma cells in Unc93b1-knockout mice compared to WT mice (Figures 7D–7G, S7K, and S7L). Together, these data show that endosomal TLRs are needed to respond to ACs in the presence of αGalCer stimulation, and in their absence, there are fewer iNKTfh cells and lower antibody responses.

DISCUSSION

SLE is characterized by autoantibodies to self-antigens that are exposed to dying cells. The patients go through flares of disease where pathological memory is being activated by various triggers. The autoreactive memory B cells have switched and gone through affinity maturation in the GC, where they receive T cell help. Here, we investigate the dynamics between conventional and unconventional T cell help when B cell tolerance is broken using injections of ACs. We found that ACs alone did not generate *i*NKTfh cells, and we have previously shown that in this response, *i*NKT cells are activated to negatively regulate the response.[19] Here, we induced *i*NKTfh cells using the exogenous ligands αGalCer and OCH and found that there was a balance between Tfh and *i*NKTfh cell recruitment where the combination activated fewer cells of both populations. Injecting glycolipids alone caused a short-lived immature GC response with the generation of *i*NKfh cells and very few Tfh cells. To further investigate the dynamics and relation between *i*NKTfh and Tfh cells, we sequenced the TCR repertoire of these populations and compared the responses. We found that overall, the greatest level of TCR (CDR3β) sharing within the Tfh population occurred between stimulations with ACs or combo. We did not observe complete sharing, and this may have been caused by incomplete sampling or a contribution from *i*NKTfh cells,

Figure 6. Co-administration of apoptotic cells and αGalCer induces an autoimmune response in a CD1d-dependent manner

(A) Experimental scheme. Age-matched *Cd1d*$^{fl/fl}$ and *Cd1d*$^{fl/fl}$*Mb1*cre mice were co-administered i.v. with mixed AC and αGC. Spleens were collected 3 days after the last injection. *Cd1d*$^{fl/fl}$ mice did not receive any injection and serve as the littermate controls in experimental setups involving *Cd1d*$^{fl/fl}$*Mb1*cre mice.

(B) The frequency of GC B cells.

(C) The frequency of *i*NKTfh cells.

(D) The frequency of plasma cells.

(E–G) The frequency of IgM$^+$ PB (E), IgG1$^+$ PB (F), and IgG3$^+$ PB (G).

(H–J) Age-matched *Cd1d*$^{fl/fl}$ and *Cd1d*$^{fl/fl}$*Mb1*cre mice were injected i.v. with AC weekly five times and combined with 2 μg αGalCer at the 3rd and 4th injections, serum was collected 14 days after the last injection. Heat maps presenting the serological spectrum of autoreactive IgG1 antibodies against nuclear antigens (H), cytoplasmic antigens (I), and tissue-specific antigens (J).

(K) The quantification of some autoreactive IgG1 antibodies.

(L) ELISA was used to measuring the OD450 nm of IgG1 anti-cardiolipin antibodies at various time points. Data are representative of three independent experiments. *$p < 0.05$, **$p < 0.01$, and ***$p < 0.001$ (Mann-Whitney test).

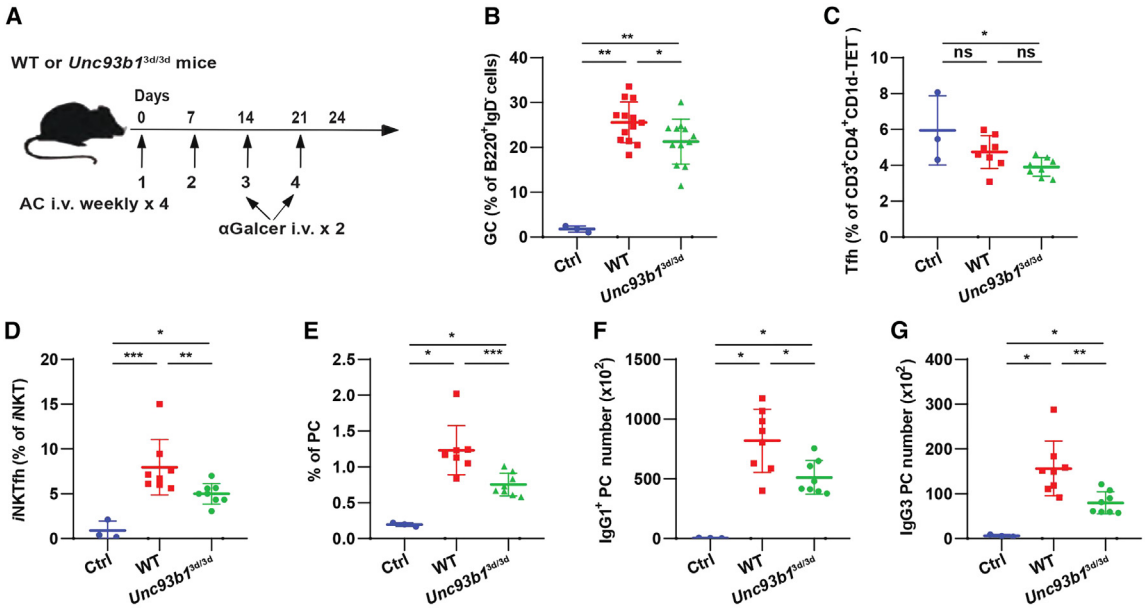

Figure 7. Endosomal pattern recognition receptors regulate *i*NKTfh cell-mediated autoimmune response

(A) Experimental scheme. Age- and sex-matched C57BL/6 wild-type and Unc93b-knockout (KO) mice were co-administered i.v. with mixed ACs and αGC four times. Spleens were collected 3 days after the last injection.

(B–D) The frequency of GC B cells (B), Tfh cells (C), and *i*NKTfh cells (D).

(E–G) The frequency or the accurate number of PCs (E), IgG1$^+$ PCs (F), and IgG3$^+$ PCs (G).

Data are representative of three independent experiments. *$p < 0.05$, **$p < 0.01$, and ***$p < 0.001$ (Mann-Whitney test).

causing new Tfh clones to arise. Thus, the addition of *i*NKTfh cells may subtly, not dramatically, reshape the pool of recruited Tfh cells during this autoreactive response. Here, we study the influence of *i*NKT cells recognizing exogenous glycolipids presented on CD1d, and in the future, it would be interesting to also investigate non-invariant type II *i*NKT cells that are reactive to sulfatide and can be enriched in certain tissues, including the CNS, kidney, and liver.[37] These cells have a more diverse TCR repertoire and have not been studied for whether they are activated to differentiate into type II *i*NKTfh cells. The activation of B cells can give rise to both GCs and extrafollicular focus, with antibody-producing cells residing in the red pulps or bridging channels. Surprisingly, we found that although there was a reduction in the individual Tfh subsets, there was an overall increase in the GC response. It has previously been shown that the limiting factor for GC size is Tfh numbers.[7] We hypothesized that adding *i*NKTfh cells would enhance the extrafollicular response in the AC group, but this was not the case. Instead, the GC response was enhanced, and we found reduced activation of IgG1-switched B cells, whereas most other subclasses were unaffected. A specific loss of the IgG1 subclass while retaining IgG2 suggests a potentially more pathogenic antibody response, as IgG1 binds preferentially to the inhibitory Fc receptor FcγRIIB. In contrast, IgG2 primarily binds activating receptors, including FcγRIV.[38] This was even more pronounced when OCH was used in combination with ACs, and this αGalCer analog has been shown to induce more IL-4 vs. IFNγ as compared to αGalCer.[39]

Future studies will determine if the shift of the B cell response is connected to cellular interactions at the border to the T cell zone, where primed T helper cells acquire the Tfh phenotype. This interaction with B cells also leads to the upregulation of AID, and recent studies have shown that switching is an early event, and thus, this decision could be made at the T-B border when B cells interact with both *i*NKTfh and Tfh cells.[40] Also, here, using conditionally targeting CD1d, we find that a cognate interaction with B cells is involved in the activation of *i*NKT cells to acquire an *i*NKTfh phenotype. The early B cell activation leading up to the GC response may be where the combined *i*NKTfh and Tfh cells influence switching and subsequent seeding of the GCs. This hypothesis is also supported by the fact that the kinetics of the *i*NKT cell-driven GC response is fast and resembles a T-independent response with plasma cells and production of mostly IgM and IgG3 antibodies.[13] Using an autoantigen array, we found that the enhanced GC response also increased autoantibody production when ACs were injected together with αGalCer. Many of the reactivities of the antibodies were similar to those found in patients with SLE and included anti-histone and complement-specific antibodies, which show that we are investigating relevant B cell responses in this study. There was no clear pattern with a boost of a specific reactivity, and instead, the induction of *i*NKTfh cells gave a general increase of autoreactive B cells across the board of specificities. This increase of autoreactivity was also dependent on cognate *i*NKT-B cells, and the boost of autoantibodies was lost when CD1d was knocked out specifically on B cells.

Here, we find a previously undescribed competition between the activation and recruitment of *i*NKTfh and Tfh cells in the autoimmune response induced by ACs. For Tfh cells, the initial activation includes interactions with DCs that present peptides on MHC class II, and DCs can also present glycolipids to activate *i*NKT cells. It has been shown previously that *i*NKT cells can modulate DC function in recruiting Tfh cells and thus modify B cells in a non-cognate manner. DCs express CD1d to a different degree depending on the subpopulations, and in mice, the highest expression is by CD8-positive DCs. These DCs are known to be good at cross-presentation, and it will be interesting to investigate whether initial *i*NKTfh cell recruitment is connected to this subset.[41,42] Another recent finding is that the sterile activation of *i*NKT cells can be performed by DCs through the generation of modified glycolipids through ER stress.[11] In this study, we describe that B cells can also rapidly respond in this way and activate *i*NKT cells *in vitro* when submitted to ER stress. Since the response to ACs is connected to cellular stress responses, this mechanism may affect *i*NKT cell activation. Future studies will determine how stress-related presentation on CD1d is connected to autoimmunity and SLE development and possible flares of disease and if it could be associated with infections. At the moment, the identity of self-glycolipids remains poorly characterized, and they could originate from both ligands derived from ACs and cellular stress responses, respectively. Collectively, in autoimmune disease, the role of *i*NKT cells can be a double-edged sword depending on the activation of *i*NKT cell subsets and their interaction with APCs. *i*NKT cells can restrict the activation of autoreactive B cells after AC injections alone, and similarly, in experimental arthritis, *i*NKT cells produce IFN-γ to limit the Th1- and Th17-mediated pathogenic response.[19,43] In their disease-promoting role described here, *i*NKT cells enable differentiation into *i*NKTfh cells after glycolipid stimulation, promoting the autoreactive IgE in an IL-18-induced antibody response.[14] Since most of the disease-promoting activity is connected to B cell activation through *i*NKTfh cell activation, it will be essential to determine how *i*NKT cells get recruited into this pool. If this choice can be modulated, it could be the base for clinically relevant treatments to steer *i*NKT cell populations toward regulating and blocking autoimmunity.

Limitations of the study

A limitation of this study is that we, so far, have not investigated spontaneous genetic models of autoimmunity. It would be of interest to see if the activation of *i*NKTfh cells would also affect the breaking of B cell tolerance in these models. In addition, we use two synthetic ligands for *i*NKT cell activation. In patients with SLE, it is likely that these would come from cellular stress responses or infection. Thus, it would be of interest to especially test if *i*NKTfh cells would be generated and regulate autoreactive B cell responses in connection to an infection.

RESOURCE AVAILABILITY

Lead contact

Requests for information regarding this study and resources should be directed to and will be handled by the lead contact, Mikael C.I. Karlsson (mikael.karlsson@ki.se).

Materials availability

Requests for resources and reagents should be directed to the lead contact, Mikael C.I. Karlsson (mikael.karlsson@ki.se).

Data and code availability

- TCR sequencing data are available from the lead contact upon request.
- This paper does not report the original code.
- Any additional information needed to reanalyze the data reported herein is available from the lead contact upon request.

ACKNOWLEDGMENTS

We thank Manasa Garimella for technical assistance and Dr. Bruce Beutler and TSRI for providing the Unc93b1$^{3d/3d}$ mice. We also would like to thank Rikard Holmdahl, Lars Nitschke, and Fredrik Wermeling for their critical review of the manuscript and experimental assistance, as well as the core facility at NEO, BEA (Bioinformatics and Expression Analysis), which is supported by the board of research at the Karolinska Institute and the research committee at the Karolinska Hospital. This study was supported by the Gustav V 80-Years Foundation and the Swedish Research Council.

AUTHOR CONTRIBUTIONS

Study concept and design, C.H., C.C., M.B., A.R.R., F.D.B., P.B., M.G., and M.C.I.K.; experimentation, C.H., S.W., S.P, M.M., G.C., Q.-Z.L., A.D.M.M., and C.C.; writing and editing, C.H., S.W., S.P., A.D.M.M., A.R.R., C.C., M.B., F.D.B., P.B., M.G., and M.C.I.K.

DECLARATION OF INTERESTS

The authors declare no conflicts of interest.

STAR★METHODS

Detailed methods are provided in the online version of this paper and include the following:

- KEY RESOURCES TABLE
- EXPERIMENTAL MODEL AND STUDY PARTICIPANT DETAILS
  - Mice
- METHOD DETAILS
  - Confocal microscopy
  - Injections
  - Flow cytometry (FACS) and antibodies
  - Immunoglobulin detection in plasma by ELISA
  - Autoantigen microarray
  - Induction of IL-2 secretion by B cells *in vitro*
  - TCR repertoire sequencing
  - TCR repertoire analysis
- QUANTIFICATION AND STATISTICAL ANALYSIS

SUPPLEMENTAL INFORMATION

Supplemental information can be found online at https://doi.org/10.1016/j.celrep.2025.115602.

Received: August 22, 2023
Revised: February 26, 2025
Accepted: March 31, 2025
Published: April 18, 2025

REFERENCES

1. Nemazee, D.A., and Bürki, K. (1989). Clonal deletion of B lymphocytes in a transgenic mouse bearing anti-MHC class I antibody genes. Nature *337*, 562–566.

2. Hartley, S.B., Crosbie, J., Brink, R., Kantor, A.B., Basten, A., and Goodnow, C.C. (1991). Elimination from peripheral lymphoid tissues of self-reactive B lymphocytes recognizing membrane-bound antigens. Nature *353*, 765–769.
3. Benner, R., Hijmans, W., and Haaijman, J.J. (1981). The bone marrow: the major source of serum immunoglobulins, but still a neglected site of antibody formation. Clin. Exp. Immunol. *46*, 1–8.
4. Kosco, M.H., Burton, G.F., Kapasi, Z.F., Szakal, A.K., and Tew, J.G. (1989). Antibody-forming cell induction during an early phase of germinal centre development and its delay with ageing. Immunology *68*, 312–318.
5. Elsner, R.A., and Shlomchik, M.J. (2020). Germinal Center and Extrafollicular B Cell Responses in Vaccination, Immunity, and Autoimmunity. Immunity *53*, 1136–1150.
6. Vinuesa, C.G., Tangye, S.G., Moser, B., and Mackay, C.R. (2005). Follicular B helper T cells in antibody responses and autoimmunity. Nat. Rev. Immunol. *5*, 853–865.
7. Victora, G.D., and Nussenzweig, M.C. (2022). Germinal Centers. Annu. Rev. Immunol. *40*, 413–442.
8. Ise, W., and Kurosaki, T. (2021). Plasma cell generation during T-cell-dependent immune responses. Int. Immunol. *33*, 797–801.
9. Chang, Y.J., Kim, H.Y., Albacker, L.A., Lee, H.H., Baumgarth, N., Akira, S., Savage, P.B., Endo, S., Yamamura, T., Maaskant, J., et al. (2011). Influenza infection in suckling mice expands an NKT cell subset that protects against airway hyperreactivity. J. Clin. Investig. *121*, 57–69.
10. Gaya, M., Barral, P., Burbage, M., Aggarwal, S., Montaner, B., Warren Navia, A., Aid, M., Tsui, C., Maldonado, P., Nair, U., et al. (2018). Initiation of Antiviral B Cell Immunity Relies on Innate Signals from Spatially Positioned NKT Cells. Cell *172*, 517–533.e20.
11. Bedard, M., Shrestha, D., Priestman, D.A., Wang, Y., Schneider, F., Matute, J.D., Iyer, S.S., Gileadi, U., Prota, G., Kandasamy, M., et al. (2019). Sterile activation of invariant natural killer T cells by ER-stressed antigen-presenting cells. Proc. Natl. Acad. Sci. USA *116*, 23671–23681.
12. Chen, Z., Zhu, S., Wang, L., Xie, D., Zhang, H., Li, X., Zheng, X., Du, Z., Li, J., and Bai, L. (2018). Memory Follicular Helper Invariant NKT Cells Recognize Lipid Antigens on Memory B Cells and Elicit Antibody Recall Responses. J. Immunol. *200*, 3117–3127.
13. Chang, P.P., Barral, P., Fitch, J., Pratama, A., Ma, C.S., Kallies, A., Hogan, J.J., Cerundolo, V., Tangye, S.G., Bittman, R., et al. (2011). Identification of Bcl-6-dependent follicular helper NKT cells that provide cognate help for B cell responses. Nat. Immunol. *13*, 35–43.
14. Sedimbi, S.K., Hägglöf, T., Garimella, M.G., Wang, S., Duhlin, A., Coelho, A., Ingelshed, K., Mondoc, E., Malin, S.G., Holmdahl, R., et al. (2020). Combined proinflammatory cytokine and cognate activation of invariant natural killer T cells enhances anti-DNA antibody responses. Proc. Natl. Acad. Sci. USA *117*, 9054–9063.
15. Tonti, E., Galli, G., Malzone, C., Abrignani, S., Casorati, G., and Dellabona, P. (2009). NKT-cell help to B lymphocytes can occur independently of cognate interaction. Blood *113*, 370–376.
16. Hagglof, T., Sedimbi, S.K., Yates, J.L., Parsa, R., Salas, B.H., Harris, R.A., Leadbetter, E.A., and Karlsson, M.C. (2016). Neutrophils license iNKT cells to regulate self-reactive mouse B cell responses. Nat. Immunol. *17*, 1407–1414.
17. Leadbetter, E.A., and Karlsson, M.C.I. (2021). Invariant natural killer T cells balance B cell immunity. Immunol. Rev. *299*, 93–107.
18. Cho, Y.N., Kee, S.J., Lee, S.J., Seo, S.R., Kim, T.J., Lee, S.S., Kim, M.S., Lee, W.W., Yoo, D.H., Kim, N., and Park, Y.W. (2011). Numerical and functional deficiencies of natural killer T cells in systemic lupus erythematosus: their deficiency related to disease activity. Rheumatology *50*, 1054–1063.
19. Wermeling, F., Lind, S.M., Jordö, E.D., Cardell, S.L., and Karlsson, M.C.I. (2010). Invariant NKT cells limit activation of autoreactive CD1d-positive B cells. J. Exp. Med. *207*, 943–952.
20. Merkenschlager, J., Finkin, S., Ramos, V., Kraft, J., Cipolla, M., Nowosad, C.R., Hartweger, H., Zhang, W., Olinares, P.D.B., Gazumyan, A., et al. (2021). Dynamic regulation of TFH selection during the germinal centre reaction. Nature *591*, 458–463.
21. Mevorach, D., Zhou, J.L., Song, X., and Elkon, K.B. (1998). Systemic exposure to irradiated apoptotic cells induces autoantibody production. J. Exp. Med. *188*, 387–392.
22. Parekh, V.V., Singh, A.K., Wilson, M.T., Olivares-Villagómez, D., Bezbradica, J.S., Inazawa, H., Ehara, H., Sakai, T., Serizawa, I., Wu, L., et al. (2004). Quantitative and qualitative differences in the in vivo response of NKT cells to distinct alpha- and beta-anomeric glycolipids. J. Immunol. *173*, 3693–3706.
23. Suurmond, J., and Diamond, B. (2015). Autoantibodies in systemic autoimmune diseases: specificity and pathogenicity. J. Clin. Investig. *125*, 2194–2202.
24. Haynes, N.M., Allen, C.D.C., Lesley, R., Ansel, K.M., Killeen, N., and Cyster, J.G. (2007). Role of CXCR5 and CCR7 in follicular Th cell positioning and appearance of a programmed cell death gene-1high germinal center-associated subpopulation. J. Immunol. *179*, 5099–5108.
25. Crotty, S. (2014). T follicular helper cell differentiation, function, and roles in disease. Immunity *41*, 529–542.
26. Jacobsen, J.T., Hu, W., R Castro, T.B., Solem, S., Galante, A., Lin, Z., Allon, S.J., Mesin, L., Bilate, A.M., Schiepers, A., et al. (2021). Expression of Foxp3 by T follicular helper cells in end-stage germinal centers. Science *373*, eabe5146.
27. Bournazos, S., Gupta, A., and Ravetch, J.V. (2020). The role of IgG Fc receptors in antibody-dependent enhancement. Nat. Rev. Immunol. *20*, 633–643.
28. Garimella, M.G., He, C., Chen, G., Li, Q.Z., Huang, X., and Karlsson, M.C.I. (2021). The B cell response to both protein and nucleic acid antigens displayed on apoptotic cells are dependent on endosomal pattern recognition receptors. J. Autoimmun. *117*, 102582.
29. Verthelyi, D., and Ansar Ahmed, S. (1997). Characterization of estrogen-induced autoantibodies to cardiolipin in non-autoimmune mice. J. Autoimmun. *10*, 115–125.
30. Lorenzo, C., Delgado, P., Busse, C.E., Sanz-Bravo, A., Martos-Folgado, I., Bonzon-Kulichenko, E., Ferrarini, A., Gonzalez-Valdes, I.B., Mur, S.M., Roldán-Montero, R., et al. (2021). ALDH4A1 is an atherosclerosis auto-antigen targeted by protective antibodies. Nature *589*, 287–292.
31. Dempsey, P.W., Allison, M.E., Akkaraju, S., Goodnow, C.C., and Fearon, D.T. (1996). C3d of complement as a molecular adjuvant: bridging innate and acquired immunity. Science *271*, 348–350.
32. Prokopec, K.E., Georgoudaki, A.M., Sohn, S., Wermeling, F., Grönlund, H., Lindh, E., Carroll, M.C., and Karlsson, M.C.I. (2016). Cutting Edge: Marginal Zone Macrophages Regulate Antigen Transport by B Cells to the Follicle in the Spleen via CD21. J. Immunol. *197*, 2063–2068.
33. Testi, R., D'Ambrosio, D., De Maria, R., and Santoni, A. (1994). The CD69 receptor: a multipurpose cell-surface trigger for hematopoietic cells. Immunol. Today *15*, 479–483.
34. Vilanova, M., Tavares, D., Ferreira, P., Oliveira, L., Nóbrega, A., Appelberg, R., and Arala-Chaves, M. (1996). Role of monocytes in the up-regulation of the early activation marker CD69 on B and T murine lymphocytes induced by microbial mitogens. Scand. J. Immunol. *43*, 155–163.
35. Fenton, K. (2015). The effect of cell death in the initiation of lupus nephritis. Clin. Exp. Immunol. *179*, 11–16.
36. Lee, B.L., Moon, J.E., Shu, J.H., Yuan, L., Newman, Z.R., Schekman, R., and Barton, G.M. (2013). UNC93B1 mediates differential trafficking of endosomal TLRs. Elife *2*, e00291.
37. Cardell, S., Tangri, S., Chan, S., Kronenberg, M., Benoist, C., and Mathis, D. (1995). CD1-restricted CD4+ T cells in major histocompatibility complex class II-deficient mice. J. Exp. Med. *182*, 993–1004.
38. Nimmerjahn, F., Bruhns, P., Horiuchi, K., and Ravetch, J.V. (2005). FcgammaRIV: a novel FcR with distinct IgG subclass specificity. Immunity *23*, 41–51.

39. Qiao, X., Xie, X., Jiang, S., Shi, W., Tang, J., and Zhou, N. (2012). Experimental bone marrow failure in mice ameliorated by OCH via tippling the balance of released cytokines from Th1 to Th2. Immunopharmacol. Immunotoxicol. *34*, 491–498.

40. Roco, J.A., Mesin, L., Binder, S.C., Nefzger, C., Gonzalez-Figueroa, P., Canete, P.F., Ellyard, J., Shen, Q., Robert, P.A., Cappello, J., et al. (2019). Class-Switch Recombination Occurs Infrequently in Germinal Centers. Immunity *51*, 337–350.e7.

41. Bai, L., Deng, S., Reboulet, R., Mathew, R., Teyton, L., Savage, P.B., and Bendelac, A. (2013). Natural killer T (NKT)-B-cell interactions promote prolonged antibody responses and long-term memory to pneumococcal capsular polysaccharides. Proc. Natl. Acad. Sci. USA *110*, 16097–16102.

42. Cavallari, M., Stallforth, P., Kalinichenko, A., Rathwell, D.C.K., Gronewold, T.M.A., Adibekian, A., Mori, L., Landmann, R., Seeberger, P.H., and De Libero, G. (2014). A semisynthetic carbohydrate-lipid vaccine that protects against S. pneumoniae in mice. Nat. Chem. Biol. *10*, 950–956.

43. Chistiakov, D.A., Sobenin, I.A., Revin, V.V., Orekhov, A.N., and Bobryshev, Y.V. (2014). Mitochondrial aging and age-related dysfunction of mitochondria. BioMed Res. Int. *2014*, 238463.

44. Metsalu, T., and Vilo, J. (2015). ClustVis: a web tool for visualizing clustering of multivariate data using Principal Component Analysis and heatmap. Nucleic Acids Res. *43*, W566–W570. https://doi.org/10.1093/nar/gkv468.

45. Tabeta, K., Hoebe, K., Janssen, E.M., Du, X., Georgel, P., Crozat, K., Mudd, S., Mann, N., Sovath, S., Goode, J., et al. (2006). The Unc93b1 mutation 3d disrupts exogenous antigen presentation and signaling via Toll-like receptors 3, 7 and 9. Nat. Immunol. *7*, 156–164.

46. Li, Q.Z., Zhou, J., Wandstrat, A.E., Carr-Johnson, F., Branch, V., Karp, D.R., Mohan, C., Wakeland, E.K., and Olsen, N.J. (2007). Protein array autoantibody profiles for insights into systemic lupus erythematosus and incomplete lupus syndromes. Clin. Exp. Immunol. *147*, 60–70.

STAR★METHODS

KEY RESOURCES TABLE

REAGENT or RESOURCE	SOURCE	IDENTIFIER
Antibodies		
CD45R/B220 PB (Clone RA3-6B2)	Biolegend	Cat#103227; RRID: AB_492876
CD169 APC (Clone 3D6.112)	Biolegend	Cat#142408; RRID: AB_2563620
GL7 FITC (Clone GL7)GL7	BD Biosciences	Cat#553666; RRID: AB_394981
CD138 APC (Clone 281-2)	Biolegend	Cat#142506; RRID:AB_10960141
IgG1 PE (Clone A85-1)	BD Biosciences	Cat#550083; RRID: AB_393553
purified CD16/32 (Clone 2.4G2)	BD Biosciences	Cat#553141; RRID: AB_394656
CD1d PE (Clone 1B1)	Biolegend	Cat#123510; RRID: AB_1236538
CD3 BV711 (Clone 17A2)	Biolegend	Cat#100241; RRID: AB_2563945
CD4 PB (Clone RM4-5)	BD Biosciences	Cat#558107; RRID: AB_397030
CD40L PerCP-Cy5.5 (Clone MR1)	Biolegend	Cat#106514; RRID: AB_2563498
CD95 PE-Cy7 (Clone Jo2)	BD Biosciences	Cat#557653; RRID: AB_396768
CD138 PE-Cy7 (Clone 281-2)	Biolegend	Cat#142514; RRID: AB_2562197
CD45R/B220 BV421 (Clone RA3-6B2)	BD Biosciences	Cat# 562922; RRID: AB_2737894
CD45R/B220 V500 (Clone RA3-6B2)	BD Biosciences	Cat#561226; RRID:AB_10584334
IgD APC (Clone 11-26c.2a)	Biolegend	Cat#405714; RRID:AB_10645480
GL-7 FITC (Clone GL7)	BD Biosciences	Cat#553666; RRID: AB_394981
PD-1 APC (Clone RMP1-30)	Biolegend	Cat#109112; RRID:AB_10613470
CXCR5 PE-Cy7 (Clone 2G8)	BD Biosciences	Cat#560617; RRID: AB_1727521
CD21 PerCP-Cy5.5 (Clone 7E9)	Biolegend	Cat#123416; RRID: AB_1595490
CD23 PE (Clone B3B4)	Biolegend	Cat#101608; RRID: AB_312832
Biotin CD9 (Clone KMC8)	BD Biosciences	Cat#558749; RRID: AB_397103
CD69 PE-Cy7 (Clone H1.2F3)	Biolegend	Cat#104512; RRID: AB_493564
CD80 BV421 (Clone 16-10A1)	BD Biosciences	Cat#562611; RRID: AB_2737675
CD8a PE (Clone 53-6.7)	Biolegend	Cat#100707; RRID: AB_312747
CD11b V711 (Clone M1/70)	Biolegend	Cat#101242; RRID: AB_2563310
CD11c PE-Cy7 (Clone HL3)	BD Biosciences	Cat#558079; RRID: AB_647251
CD86 AF700 (Clone GL-1)	Biolegend	Cat#105024; RRID: AB_493720
Biotin CD86 (Clone GL-1)	Biolegend	Cat# 105003; RRID: AB_313146
I-A/I-E PE (Clone M5/114.15.2)	BD Biosciences	Cat# 557000;RRID:AB_11151902
CD25 PE-Cy7 (Clone PC61)	BD Biosciences	Cat#552880; RRID: AB_394509
NK1.1 PerCP-Cy5.5 (Clone PK136)	Biolegend	Cat#108728; RRID: AB_2132705
IgM APC (Clone RMM-1)	Biolegend	Cat#406509; RRID: AB_315059
IgG1 PE (Clone A85-1)	BD Biosciences	Cat#550083; RRID: AB_393553
IgG2b FICT (Clone R12-3)	BD Biosciences	Cat#553395; RRID: AB_394833
IgG3 BV605 (Clone R40-82)	BD Biosciences	Cat#744135; RRID: AB_2742024
Bcl-6 APC-Cy7 (Clone K112-91)	BD Biosciences	Cat#563581; RRID: AB_2738291
GATA-3 PB (Clone L50-823)	BD Biosciences	Cat#563349; RRID: AB_2738152
T-bet PE-Cy7 (Clone 4B10)	Biolegend	Cat#644824; RRID: AB_2561760
HRP-conjugated IgM	SouthernBiochem	Cat#1020-05
HRP-conjugated IgG	SouthernBiochem	Cat#1030-05
HRP-conjugated IgG1	SouthernBiochem	Cat#1070-05
HRP-conjugated IgG2b	SouthernBiochem	Cat#1090-05
HRP-conjugated IgG2c	SouthernBiochem	Cat#1078-05
HRP-conjugated IgG3	SouthernBiochem	Cat#1100-05

(*Continued on next page*)

Continued

REAGENT or RESOURCE	SOURCE	IDENTIFIER
Streptavidin Qdot™ 605	Thermo Fisher Scientific	Cat#Q10101MP
Chemicals, peptides, and recombinant proteins		
proLong™ diamond antifade mountant	Invitrogen	Cat#P36961
Dexamethasone	Sigma-Aldrich	Cat# D2915
αGalCer	AdipoGen Life Sciences	Cat# AG-CN2-0013-M001
PBS-57 loaded CD1d tetramers PE	NIH Tetramer Core Facility	Cat#37365
OCH	NIH tetramer core facility	N/A
dimethyl sulfoxide	Sigma-Aldrich	Cat# D2438
NP-CGG	Biosearch Technologies	Cat# N-5055D-5
Cardiolipin	Sigma-Aldrich	Cat# C1649
ALDH4A1-Flag	Almudena R. Ramiro's lab	N/A
IKAROS–Flag protein	Almudena R. Ramiro's lab	N/A
Gelatin	Sigma-Aldrich	Cat# G2500
BSA	Sigma-Aldrich	Cat#05470
NP2-BSA	Biosearch Technologies	Cat# N-5050M-10
NP36-BSA	Biosearch Technologies	Cat# N-5055D-5
RPMI medium	Gibco™	Cat#11875093
FBS	HyClone	Cat# SV30160.03HI
penicillin-streptomycin	HyClone	Cat# SV30010
sodium pyruvate	Sigma-Aldrich	Cat# S8636
2-mercaptoethanol	Gibco™	Cat#21985-023
Thapsigargin	Invitrogen	Cat# T7459
Critical commercial assays		
live/dead fixable stain kit	Invitrogen	Cat# L34955
fixation/permeabilization solution kit	BD Biosciences	Cat#554714
Foxp3/Transcription Factor Staining Buffer Set	eBioscience	Cat#00-5523-00
TMB substrate	Biolegend	Cat#421101
B Cell Isolation Kit, mouse	Miltenyi	Cat#130-090-862)
Mouse IL-2 ELISA BASIC kit	MABTECH	Cat# 3441-1H-6
Pan T Cell Isolation Kit II	Miltenyibiotec	Cat#130-095-130
Software and algorithms		
FlowJo 10	FLOWJO, LLC	https://www.flowjo.com
Prism 8.0	GraphPad software	https://www.graphpad.com/scientific-software/prism/
BD FACSDiva	BD Biosciences	https://www.bdbiosciences.com/en-us/products/software/instrument-software/bd-facsdiva-software
ImageJ		https://imagej.net/
ClustVis	BIIT ClustVis	Metsalu and Vilo[44]
MiXCR-3.0.13	MiLaboratories Inc	https://mixcr.readthedocs.io/en/master/
R	R Foundation	r-project.org
Immunarch package		https://CRAN.R-project.org/package=immunarch
ggvenn		https://cran.r-project.org/web/packages/ggvenn/index.html
ggplot2		https://ggplot2-book.org/

EXPERIMENTAL MODEL AND STUDY PARTICIPANT DETAILS

Mice

All mice were on the C57BL/6 background and mice and backcrossed at least 12 generations. *Mb1cre* mice were obtained from Charles River and Jackson Laboratories. *Cd1d*$^{fl/fl}$ mice were generated by Facundo D. Batista (Ragon Institute, USA).[10] Unc93b1 (3d/3d) mice were a kind gift from Dr. Bruce Beutler.[45] Wild type control littermates were bred from the same backcrosses in all experimental setups. Mice were age (8-10 weeks) and sex matched within each experiment and no differences were detected in

connection to sex or age in the experiments performed. All mice were housed at SPF conditions and animal experiments were performed according to the protocols described in ethical permits (no: 14304-23 and 5377-2018) of Mikael Karlsson and approved by the Stockholm North Animal Ethics committee and Stockholm North district court.

At indicated time points, serum was collected from the tail vein and mice were sacrificed for analysis. All animal experiments were performed according to the protocols described in ethical permits (11159/18 and 05294-2023) of L. Westerberg, approved by the Stockholm North Animal Ethics Committee (Stockholm, Sweden).

METHOD DETAILS

Confocal microscopy

For spleen staining, GCs were visualized by staining with conjugated antibodies directed against B220, CD169 and GL-7. Plasma cells were detected by conjugated antibodies against B220, CD138, and IgG1. Washed slides were mounted with proLong™ diamond antifade mountant (Invitrogen). Visual data were acquired with a confocal microscope LSM880 (Zeiss) and recorded with the LSM Image software. Images were analyzed with Photoshop. The number of *i*NKT cells in germinal centers (GCs) and the area of germinal centers (GCs) were quantified using ImageJ.

Injections

Apoptotic cells were made from thymocytes from 4-5 weeks C57BL/6 old mice, which were cultured in 1 μM dexamethasone (Sigma-Aldrich) RPMI 1640 media for 12 h. Twenty million cells were injected, i.v. weekly for 4-5 times. αGalCer (AdipoGen Life Sciences) and OCH (from NIH tetramer core facility) was prepared in dimethyl sulfoxide (Sigma-Aldrich) diluted in PBS with a final DMSO concentration of lower than 0.5%. Two μg of αGalCer or OCH were injected i.v. with 3rd and 4th AC injections. Blood was collected from the ventral tail artery. For the humoral immune response, mice were immunized intraperitoneally with 100 μg NP-CGG (Biosearch Technologies) with two μg of αGalCer or OCH injected intravenously according to the groups. Serum was collected on the indicated time points.

Flow cytometry (FACS) and antibodies

Cells were Fc-blocked with purified anti-mouse CD16/32 (BD Biosciences) to reduce unspecific binding and stained with live/dead fixable stain kit (Invitrogen) to exclude dead cells. They were then stained the appropriate combination of fluorochrome-conjugated surface antibodies. Cells were fixed with fixation/permeabilization solution kit (BD Biosciences) or Foxp3/Transcription Factor Staining Buffer Set (eBioscience) and followed with cytosol staining or nuclear staining. The antibodies used in this study are listed in the key resources table. Samples were acquired in the LSRFortessa™X-20 (BD Biosciences) and analyzed with FlowJo ver. 10 software (BD Biosciences). Dead cells were excluded from analysis by side/forward scatter gating.

Immunoglobulin detection in plasma by ELISA

ELISA plates were coated with 100 μL 20ug/mL cardiolipin (Sigma-Aldrich) in 99.9% ethanol, overnight to detect cardiolipin-specific antibodies. Plates were blocked with 10% FBS in PBS for 1 h at 37°C and incubated with 1:100 diluted serum from mice for 1 h at 37°C. For the ALDH4A1 test, plates were coated with 5 μg/ml ALDH4A1-Flag or IKAROS–Flag protein (generated by Almudena R. Ramiro's lab) ELISA plates were coated with 100 μL 20ug/mL cardiolipin (Sigma-Aldrich) in 99.9% ethanol, overnight to detect cardiolipin-specific antibodies. Plates were blocked with 10% FBS in PBS for 1 h at 37°C and incubated with 1:100 diluted serum from mice for 1 h at 37°C. For the ALDH4A1 test, plates were coated with 5 μg/ml ALDH4A1-Flag or IKAROS–Flag protein (Lorenzo et al., 2021); blocked with 1% BSA and incubated with mouse plasmas (1:50 dilution for IgM, 1:10 dilution for IgG). For NP-specific ELISA, plates were incubated with 10 μg/mL NP2-BSA or NP36-BSA (Biosearch Technologies) at 4°C overnight. Washed Plates were blocked with block buffer (3 mM EDTA, 0.1% gelatin [Sigma-Aldrich], 1.5% BSA [Sigma-Aldrich] in PBS) for 2 h at RT and incubated with mouse plasma overnight. Then they were incubated with horseradish peroxidase (HRP)-conjugated secondary antibodies for 1 h at 37°C and developed with TMB substrate (Biolegend). The optical density at 450 nm (OD450) and 620 nm (OD620) was measured by an Eon Microplate Spectrophotometer (BioTek). Secondary antibodies for Elisa include HRP-conjugated goat antibody to mouse IgM, IgG, IgG_1, IgG_{2b}, IgG_{2c}, and IgG_3 (SouthernBiochem).

Autoantigen microarray

We used a microarray containing 121 autoantigens to identify the broad spectrum of autoantibodies (University of Texas Southwestern Medical Centre). Array and analyses were performed according to protocols in the genomics and microarray core facility at the University of Texas Southwestern Medical Center.[46] Net signal intensity was used to generate heat maps through ClustVis online tool.

Induction of IL-2 secretion by B cells *in vitro*

Cells were cultured at a density of 1×10^5 cells/ml in RPMI medium (GibcoTM) supplemented with 10% FBS (HyClone), 1×penicillin-streptomycin (HyClone), 1 mM sodium pyruvate (Sigma-Aldrich) and 50 μM 2-mercaptoethanol (GibcoTM) in the humidified environment at 37°C with 5% CO2. We treated 1×10^5 CH12 cells with 25 nM, 50 nM, or 100 nM thapsigargin (Invitrogen) for 3.5 h. After

treatments, cells were washed three times with a fresh medium. Then 3.3x104 DN32.D3 cells hybridomas, a mouse *i*NKT cell line, were added to the wells and cocultured overnight. For blocking experiments, CH12 cells were incubated with 25 nM thapsigargin in the presence or absence of 10 μg/ml murine anti-CD1d (Biolegend). For experiment with primary B cells from C57BL76 cells, B cells were isolated from spleen suspension using B Cell Isolation Kit, mouse (Miltenyi). The supernatant was used to detect the IL-2 secretion by Mouse IL-2 ELISA BASIC kit (MABTECH).

TCR repertoire sequencing

For each stimulation condition, splenocyte T cells were enriched by Pan T Cell Isolation Kit II, mouse (miltenyibiotec) and stained to identify Tfh ($CXCR5^+PD\text{-}1^+CD3^+CD4^+CD1d\text{-}\alpha\text{-}TET^-B220^-$) and *i*NKTfh ($CXCR5^+PD\text{-}1^+$ $CD3^{int}CD1d\text{-}\alpha\text{-}TET^+$ $B220^-$) cells. From each population, 10000 cells were sorted out using a FACSAria™ III Sorter (BD Biosciences)). We isolated total mRNA and performed library preparation for sequencing according to the Smart-seq2 protocol in bulk. Libraries were sequenced with paired-end (2x50 bp) chemistry on an Illumina NextSeq 2000 to a depth of approximately 25-30 million reads per sample at the BEA core facility (Karolinska Institutet).

TCR repertoire analysis

Unpaired TCR alpha/beta clonotypes were assembled from sequencing data using MiXCR-3.0.13 with the analyze shotgun pipeline and loaded into R using the repLoad function from the immunarch package (0.6.7). Further analyses and plots were produced in R using the following packages: immunarch (0.6.7), ggvenn (0.1.9), and ggplot2 (3.3.5). Samples from replicates were combined for analysis without any modifications such as normalization. To calculate the proportion overlap between different treatment conditions: shared clonotypes were first identified, the sum of their frequencies was calculated, and then divided by the total number of clones from both populations.

QUANTIFICATION AND STATISTICAL ANALYSIS

Prism software 8.0 was used for the analysis of graphs and data. Statistical significance was tested with the Mann-Whitney test (*$P < 0.05$, **$P < 0.01$, and ***$P < 0.001$).